Solar cycle dependence of Wind/EPACT protons, solar flares and coronal mass ejections

Miteva, R. [1], Samwel, S. W. [2], Costa-Duarte, M. V. [3], Malandraki, O. E. [4]

[1] Space Research and Technology Institute, Bulgarian Academy of Sciences, Bulgaria.
[2] National Research Institute of Astronomy and Geophysics, Helwan, Cairo, Egypt.
[3] Institute of Astronomy, Geophysics and Atmospheric Sciences, University of São Paulo, São Paulo, Brazil.
[4] Institute of Astronomy, Astrophysics, Space Applications and Remote Sensing, National Observatory of Athens, Penteli, Greece.

E-mail (rmiteva@space.bas.bg)

Accepted: 8 September 2016

Abstract The aim of this work is to compare the occurrence and overall properties of solar energetic particles (SEPs), solar flares and coronal mass ejections (CMEs) over the first seven years in solar cycles (SCs) 23 and 24. For the case of SEP events, we compiled a new proton event catalog using data from the Wind/EPACT instrument. We confirm the previously known reduction of high energy proton events in SC24 compared to the same period in SC23; our analysis shows a decrease of 25–50 MeV protons by about 30%. The similar trend is found for X to C-class solar flares which are less by about 40% and also for faster than 1000 km/s CMEs, which are reduced by about 45%. In contrast, slow CMEs are more numerous in the present solar cycle. We discuss the implications of these results for the population of SEP-productive flares and CMEs.

Keywords: solar energetic particles; solar flares; CMEs; solar cycle

1. Introduction

The historical parameter used to describe solar activity and its temporal behavior is the sunspot number. The duration of a given solar cycle (SC), however, varies slightly around the well-known 11-year period (Hathaway, 2010). With the new and improved space-borne observations in various wavelength regimes (mostly since 1996), a number of other solar phenomena could be monitored in great detail for nearly two SCs, among them are the solar flares, coronal mass ejections (CMEs) and solar energetic particles (SEPs). These constitute the main drivers of space weather (Schwenn, 2003) following the overall trend outlined by the sunspot count variation throughout the years.

SEPs (electrons, protons and heavy ions) are the enhancements of the particle intensity observed in situ that follow in time the solar eruptions, flares and CMEs. Usually, SEP events are observed at a single point in space, routinely at L1 and occasionally outside the ecliptic plane. Recent multi-spacecraft observations using the twin STEREO spacecraft (Kaiser et al. 2008) showed simultaneous SEP onsets at large longitudinal extents in the heliosphere (Gomez-Herrero et al. 2015).

Two main physical processes, namely, magnetic reconnection during solar flares and shocks driven by CMEs, can accelerate particles in the solar atmosphere and interplanetary (IP) space, respectively (Cane, Richardson, and von Rosenvinge (2010), Reames (2013) and references therein). Thus, the SEP productivity depends on the overall trend of flare and CME occurrence. The SEP-productive eruptive events, however, are small subsets of the overall flare/CME distributions. Following the acceleration, the energetic particles escape from the corona (Klein et al. 2008, Agueda et al. 2014), sustain various transport effects in the IP space before being finally detected, provided the magnetic field lines sweep over the satellite.

The quantitative comparisons of the occurrence and properties of the SEPs and their solar origin over the SC is a subject of several recent studies. Since SC24 is still ongoing, all reports are based on comparison of partial data samples. The analysis in Gopalswamy (2012) and Chandra et al. (2013) cover about 3.5 and 3 years from SC24, respectively, with about 20 events in each rise phase. Gopalswamy et al. (2014) report about 30 major SEP events in the first 5 years of SC24, whereas Mewaldt et al. (2015) extend their sample to about 5.8 years in each SC. Despite the samples limitation, several trends in SC24 could be identified: a decrease in the number of high energy particles and larger fraction of halo-CMEs resulting into SEPs (Gopalswamy 2012); poor magnetic connectivity, in longitude and latitude, and unfavorable ambient conditions (Gopalswamy et al. 2014); reduced magnetic field strength (McComas et al. 2013; Mewaldt et al. 2015), north-south asymmetry (Gopalswamy 2012; Chandra et al. 2013); reduced number of seed particles (Mewaldt et al. 2015).

The focus of this work is the solar cycle dependence of the observed near Earth proton events and the entire population of solar eruptive phenomena, flares and CMEs, irrespective of their SEP production. The 20-year behavior (1996–2015) of proton events in two energy channels is investigated here using a newly compiled Wind/EPACT proton

catalog. In this study, we extend the time period for quantitative comparison of solar phenomena in the two SCs to 7 years of observations. In addition, we employ statistical methods to quantify any difference between the two SCs. Finally, we discuss our findings in the context of SEP productivity.

2. Data analysis

2.1 Catalog of Wind/EPACT proton events

For the compilation of the proton catalog, we used omni-directional data from the Energetic Particle Acceleration, Composition, and Transport (EPACT) instrument aboard the Wind spacecraft (von Rosenvinge et al. 1995) in the energy ranges 19–28 MeV and 28–72 MeV provided by the CDAWeb database (http://cdaweb.gsfc.nasa.gov/) in the period 1996–2015. Using the possibilities of the CDAWeb database we first plotted the data in a 3-to-5 day period for a visual identification of the proton enhancements. When such enhancement was visually confirmed we then collected the proton data (over a period of several days around the approximate onset time) and performed detailed analysis, see below. The time resolution of the data is 92 seconds and the proton intensity is in $(cm^2\ s\ sr\ MeV)^{-1}$. Two examples of the intensity–time proton profiles at low (~25 MeV) and high energy (~50 MeV) are given in Figure 1. The improved statistics for the high intensity event (2013-04-11) is evident since no smoothing of the data is used. In order to achieve a comparable visibility for the low intensity event (2013-03-04), a smoothing over 20 consecutive points is performed. The protons exhibit very similar profile in the two energy channels especially for the high intensity events (see Figure 1, lower plot). Nevertheless, for the data analysis we kept the two contiguous channels as separate.

We identified about 360 proton events in the low energy channels and about 340 high energy protons. Hereafter, we will regard the entire event sample as the Wind/EPACT event catalog. A small subset (of about one quarter) from the present event list at ~25 MeV channel was analyzed in Miteva et al. (2013) as the counterparts of another SEP list.

The first version of the Wind/EPACT proton catalog (Miteva et al. 2016) is available online under: http://newserver.stil.bas.bg/SEPcatalog/index.html. The main components of the Wind/EPACT catalog are the onset time, peak proton intensity and peak time. The latter two values are usually straightforward to identify. Occasionally, a local shock-related signature is evident at 25 and/or 50 MeV intensity–time plots. In such cases, the intensity value reached just before this locally-accelerated component in the proton profiles is selected as the peak.

The pre-event intensity level (or so-called background level) is used for the determination of the proton onset time and amplitude. It is usually calculated over a quiet-time interval chosen by an observer. This introduces some subjectivity to the evaluation of the onset time. Compared to the peak intensity, the value of the background level is,

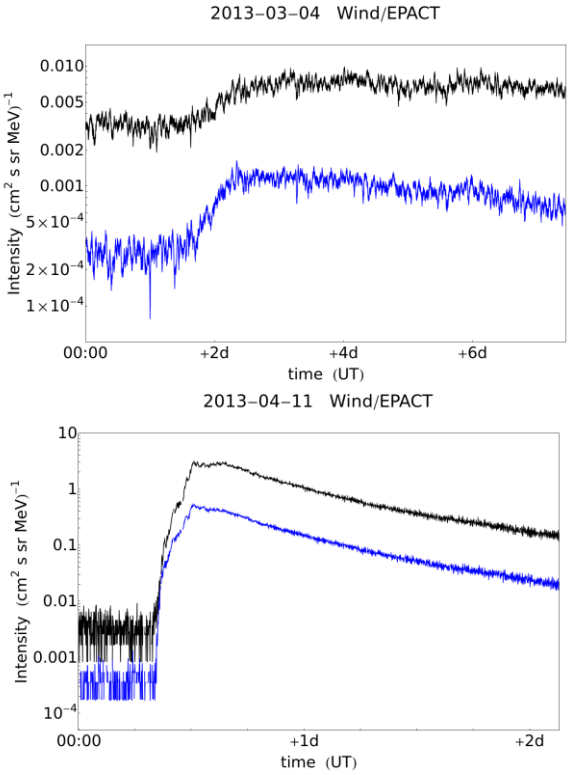

Figure 1: Example plots from Wind/EPACT ~25 MeV (black/upper) and ~50 MeV (blue/lower) for two different particle profiles plotted over several days. The event onset day is given in the plot caption.

in general, very small. However, when the new SEP increase occurs on the aftermath of an ongoing event, calculating a background subtracted peak is crucial for the correct evaluation of the SEP amplitude. Background subtracted peak intensities are reported in the Wind/EPACT catalog.

The onset time determination, however, is subject to some controversy. Usually, uncertainty ranges are not given (see, however, Miteva et al. 2014). A large part of the ambiguity is due to the choice of the SEP onset time definition. Different criteria have been used in the literature for onset time, for example: when the particle intensity level increases above the pre-event level with a range of 2 (Tylka et al. 2003) to 4 (Krucker et al. 1999) standard deviations (sigmas) used as a threshold; Poisson-CUSUM method (Huttunen-Heikinmaa, Valtonen, and Laitinen 2005); fixed threshold levels in the SEP intensity used over large periods of time (e.g., GOES proton list; SEPServer proton list), point of intersection of the pre-event intensity level with a straight-line fit to the logarithm of the particle profile (Miteva et al. 2014), etc. The specific choice is to some extent arbitrary. In addition, using either the best resolution data available (often with large amount of noise) or smoothed particle intensity (with a wide range of values selected for the averaging) will lead to a different result for the onset and the peak values.

In the Wind/EPACT proton catalog, we adopt the definition of 3-sigma value above background level applied on the 5-point smoothed data in order to calculate the onset time. The values of peak proton

intensity (denoted by J_p) and peak time are identified also from the smoothed data at the maximum of the intensity profile. Proton events with intensity profiles compromised by gaps, spikes and other data issues are dropped from the analysis.

During the same time period (1996–2015), there are other proton lists available (on-line), e.g.: GOES >10 MeV proton list (http://umbra.nascom.nasa.gov/SEP/), the SEPServer ~68 MeV proton list (http://server.sepserver.eu/), as well as the SEPEM reference proton list (http://dev.sepem.oma.be/help/event_ref.html). The latter, however, does not extend beyond March 2013 and thus is not considered in our analysis.

Each of these proton lists has different identification criteria applied. The GOES proton list adopts the 10 proton flux unit (pfu) threshold in the >10 MeV energy channel in order to report a proton event, where 1 pfu = 1 proton/(cm^2 s sr). The catalog will miss a new SEP increase that occurs during times of elevated background intensity (namely, higher than 10 pfu, as in the case of a preceding SEP event). Thus, the list is biased to strong events (since weak events < 10 pfu threshold are not reported) starting from an intensity level below 10 pfu. Any statistical study based on this catalog will consider only these SEP events.

The SEPServer event list (Vainio et al. 2013) has lower threshold criteria for the SOHO/ERNE 55–80 MeV energy channel and it reports numerous low intensity SEP events at higher energy (~68 MeV) compared to the GOES proton events. The SOHO/ERNE instrument, however, occasionally saturates for large intensity SEP events and such events are dropped from this analysis.

In Figure 2 we show the correlation plots between the peak intensity at low and high energy Wind/EPACT channels with the GOES and SEPServer proton events, respectively. The Pearson correlation coefficients (log–log) are very high in either case: we obtain correlation of 0.83 between the ~25 MeV Wind/EPACT and GOES peak proton intensities (over a sample of 123 events) and 0.82 between the ~50 MeV Wind/EPACT and SEPServer ~68 MeV protons (152 events). The results show the consistency between proton intensity trends observed with the Wind/EPACT energy channels and by other instruments with similar energy coverage.

2.2 Flare and CME catalogs

The parameters of solar flares are collected from the GOES soft X-ray (SXR) instrument reports available online:
http://hesperia.gsfc.nasa.gov/goes/goes_event_listings. The CME properties are adopted as reported from the online SOHO/LASCO CME catalog: http://cdaw.gsfc.nasa.gov/CME_list/ (Gopalswamy et al. 2009).

3. Results

Below, we outline the procedure used to deduce the SC variation of solar events: low and high energy Wind/EPACT protons, flares and CMEs, both for the overall populations and various subsets. First, we plot the overall distributions of SEP, flares and/or CME events in the entire period, 1996–2015.

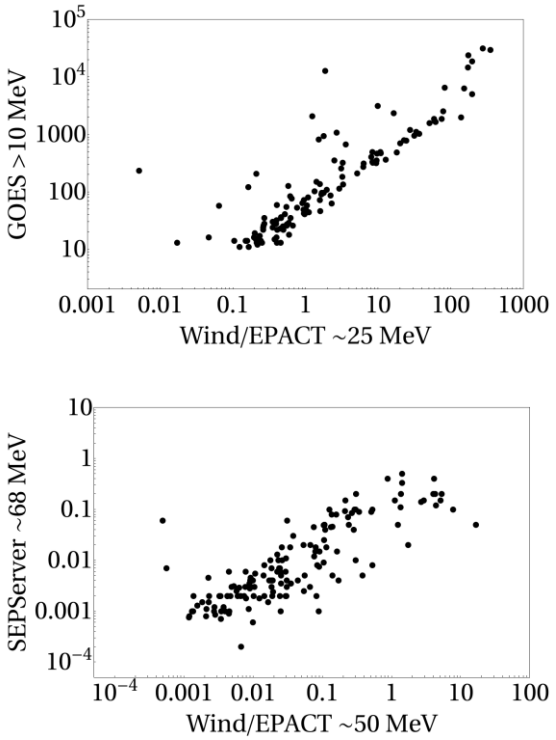

Figure 2: Upper plot: scatter plot between the peak proton intensity of Wind/EPACT low energy in (cm^2 s sr MeV)$^{-1}$ and GOES >10 MeV channel in pfu. Lower plot: scatter plot between the peak proton intensity from Wind/EPACT high energy and SEPServer ~68 MeV energy, both in (cm^2 s sr MeV)$^{-1}$.

For the quantitative comparison between the SC occurrence and properties of the different space weather agents, we require the same time period in each SC. We use the 13-month smoothed sunspot number (data from Royal Observatory of Belgium; http://www.sidc.be/silso/datafiles) to identify the minimum in the SC. We adopt the last reported minimum value before the continuous increase of the next SC, namely sunspot number of 11.2 in August 1996 and 2.2 in December 2008. As the onset of the SC we take the month following the month of the sunspot minimum. In order to take advantage of the entire well-observed period of the SC24, e.g., 01/2009–12/2015, we take the corresponding 7 year-period after the start of SC23, namely, 09/1996–08/2003.

The statistical differences between the pairs of various solar phenomena in SC23 and SC24 are tested using the Bayesian scheme, based on Kruschke (2013). Finally, as a quantitative measure for the productivity of solar protons and eruptive phenomena in SC23 and SC24 we utilize the so-called percentage change. This is the difference between the number of events in SC24 and SC23 divided to the number of events in SC23. We apply the percentage change on two different time periods. Namely we compare 6 month (for flares and CME samples) or 1 year (for the proton samples) periods from SC23 and SC24 (occurring in a succession without a temporal overlap) and in addition, we compare cumulative duration from the

onset of each SC (with a step of 1 to 1.5 years) to 7 years after each SC onset. The negative (positive) values represent a reduction (increase) of the number of events in the SC24 with respect to the event number in SC23. The uncertainty of this percentage change is calculated as a standard (Poisson) error.

3.1 Proton events

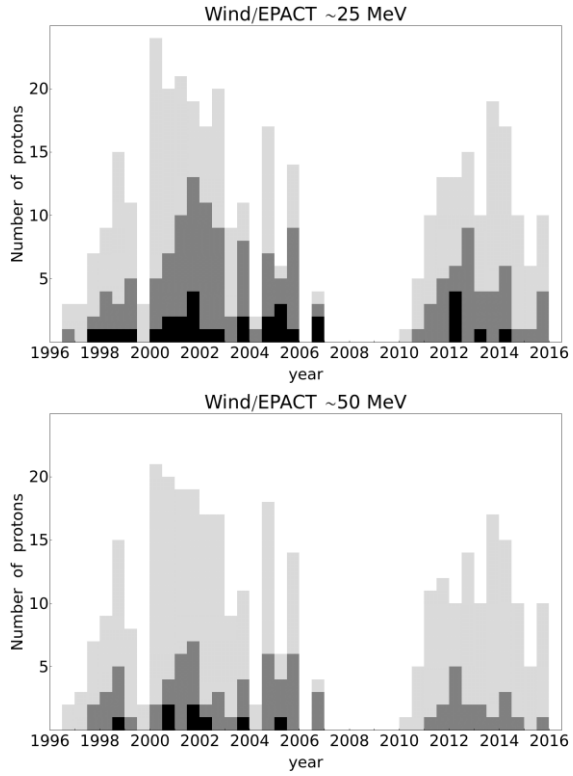

Figure 3: Distribution of the number of Wind/EPACT proton events (upper plot: low energy chanel, lower plot: high energy channel) with time. The length of the color bar gives the number of each category in a 6-month time bin. The color code denotes proton events with $J_p \geq 10$ (black), $0.1 \leq J_p < 10$ (gray) and $J_p < 0.1$ (light gray). The total number of proton events in each bin is the sum of all three colored bars.

The distributions of the Wind/EPACT peak proton intensity at low (~25 MeV) and high (~50 MeV) energy over the solar cycle are given in Figure 3. The color code denote the strength of the SEP events, defined as major ($J_p \geq 10$), medium ($0.1 \leq J_p < 10$) and minor ($J_p < 0.1$), respectively, where J_p is in $(cm^2\ s\ sr\ MeV)^{-1}$. The total number of ~25 and ~50 MeV proton events is less in the ongoing SC24. In addition, major SEP events at ~50 MeV energy channel have not been observed in this SC (as by the end of 2015).

In Table 1 we summarize the mean and median values of the proton intensity for all categories of low and high energy proton events. According to the Bayesian test, the samples of proton events observed in SC23 and SC24 are not statistically different. The values for the percentage change, calculated using the numbers of events observed in the entire 7-year time period, are given in the last column of Table 1. They consist of exclusively negative numbers, which means there is a global trend of reduction of proton events in SC24. A drop of about 30 % both in low and high energy proton events in SC24 is obtained, whereas the reduction of major intensity protons is the highest (from 60% for ~25 MeV protons to 100% for the ~50 MeV protons) and is the lowest for the minor events (as low as about 20%).

Table 1 shows the value of the percentage change averaged over the entire period of 7 years after the SC onset for the entire sample and different proton intensity categories. Any changes that occur on a smaller time scale, however, are smoothed out. In order to investigate the temporal behavior of the percentage change we used the same procedure to calculate the percentage change but applied over individual yearly time intervals starting from each SC onset. Namely, the productivity of SC23 is compared to the same period of SC24, shifted in time by one year.

Table 1: Properties of Wind/EPACT proton events for different proton intensity ranges of J_p (all, major, medium, minor) in two energy channels, during the first 7 years of SC23 and SC24. The total number of proton events in each category is given in brackets. The percentage change is positive (negative) for more (less) events observed in SC24 compared with the same period in SC23.

Categories of Wind/EPACT protons	Mean/Median SC23: 09/1996-08/2003	Mean/Median SC24: 01/2009-12/2015	Statistical difference	Change in SC24
~25 MeV protons				–29±8%
• major	75/60 (15)	44/48 (6)	No	–60±19%
• medium	0.63/0.52 (58)	0.54/0.51 (38)	No	–34±14%
• minor	0.017/0.015 (109)	0.017/0.015 (85)	No	–22±11%
~50 MeV protons				–29±8%
• major	16/14 (6)	- (0)	-	–100%
• medium	0.59/0.34 (30)	0.60/0.30 (18)	No	–40±18%
• minor	0.014/0.013 (133)	0.004/0.003 (102)	No	–23±10%

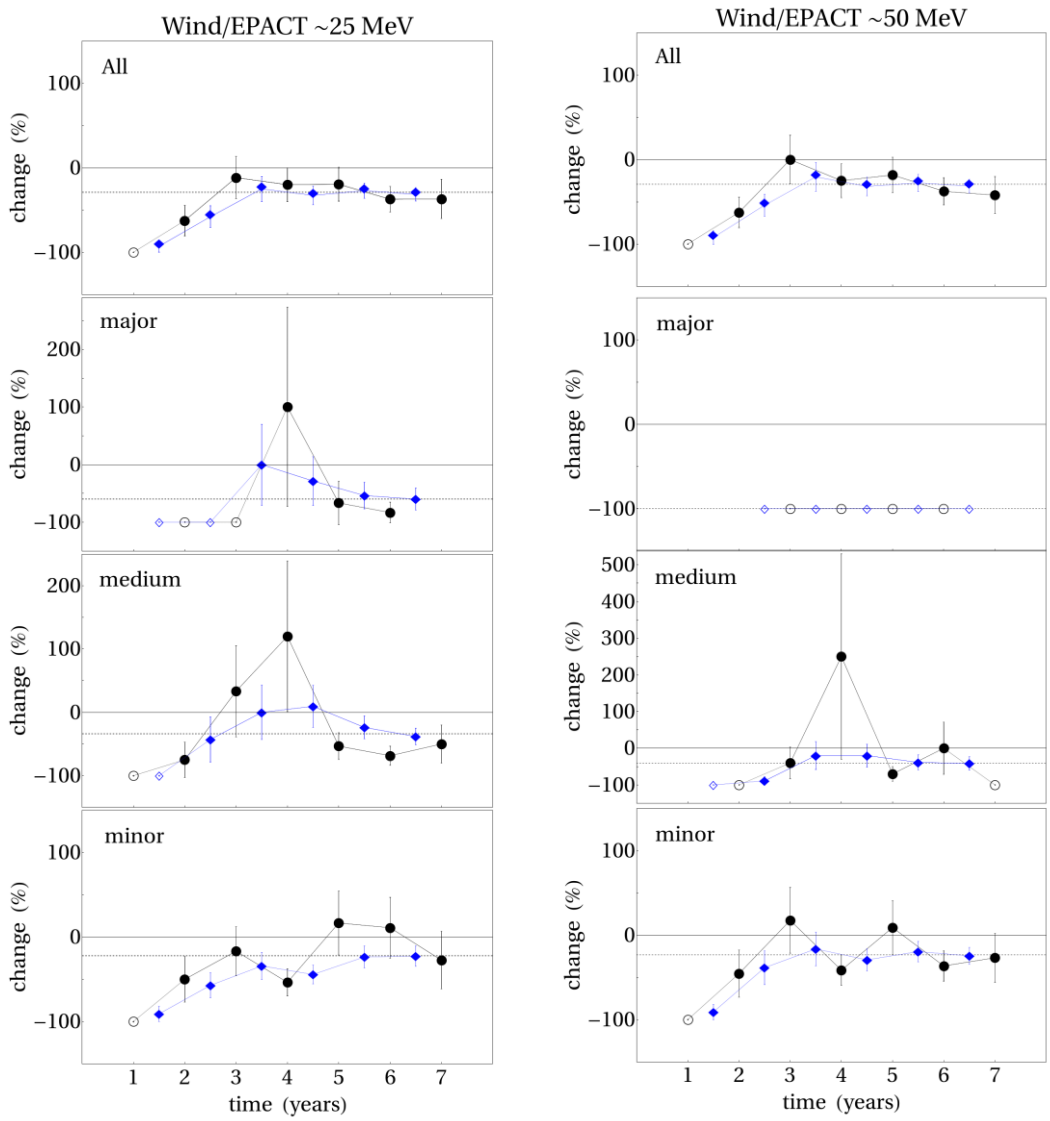

Figure 4: Plots of the yearly percentage change (black circles) and cumulative percentage change (blue diamonds) of Wind/EPACT proton events in the low (left) and high (right) energy channel. Positive (negative) values denote more (less) events in SC24 compared to SC23. Empty symbols denote a percentage change value with undetermined uncertainty due to lack of observed events in SC24. The dotted line in all plots is the respective value averaged over all 7 years (see Table 1).

The plots of the percentage change for the low and high energy protons are shown in Figure 4 with circles. In overall, there is a variation of the percentage change during the course of the SC. The trend of all proton events (notation 'All') in both energy channels is reminiscent to the behavior of their respective population of minor events that fluctuates around the 0-level (notation 'minor'). The latter two trends are also similar to each other. This is because the minor events are the most numerous sample and will dominate the distribution of all events. This is also evident while calculating mean/median values (Table 1). The behavior of the 'medium' and 'major' protons is, however, different from the minor/All proton samples. The medium/major proton subsets show a sudden short-lived (of about 1 year) rise of the proton productivity in SC24 (i.e., in 2012), compared to the same period in SC23 (e.g., in 1999–2000) that occurs about 4 years after the start of each SC. This trend is marginally significant for medium SEPs in the low energy channel, whereas the uncertainty for the major ~25 MeV SEPs is too large. Since by the end of 2015 major ~50 MeV protons have not been observed, the trend is flat in the corresponding plot. All other (positive) values have too large error margins to be significant.

The values of the cumulative percentage range are plotted on each respective plot in Figure 4 using diamond symbol. For a visibility purpose, we calculated the cumulative values of percentage change using time period of 1.5, 2.5 etc. to 6.5 years after each SC onset. Within the error margins, after about 3.5 years the percentage change is practically the same as the value obtained using 7 years of data. Namely, the

trend of the SC productivity converges to the present value after the first 3 years of the SC. We confirm that SC24 has an increased productivity for major and medium proton events at about 3.5–4.5 years after the SC onset compared to the averaged 7-year trend. However, the increase is very small and marginally significant only for medium ~25 MeV proton events. In overall, the cumulative percentage change, both for low and high energy protons, shows a smoothed trend, without the outliers exhibited by the trend based on shorter time periods.

3.2 Solar eruptive events: flares and CMEs

3.2.1 Overall behavior

In this Section, we consider the temporal behavior of entire population of observed solar flares and CMEs. We use all reported flares from 1996 to 2015 above B1-class from the GOES SXR flare listings. (The flare class denotes the peak SXR flux reached in GOES 0.1 to 0.8 nm channel, where X stands for 10^{-4} W m^{-2} and each weaker class (M, C, and B) denotes a decrease by a factor of 10. The number after the letter is a multiplication factor.) The GOES SXR listings comprise over 35 000 flare entries since 1996 and the fraction above B1-class is close to 100% from all reported flares. The distribution in the different intensity classes (X+M, C and B) is given in Figure 5 (upper plot), using 6-month binning. Different colors are used to denote the fraction of each flare class, namely, black for X and M-class, gray for C-class and light-gray for B-class flares. The total number of flares is given by the envelope (sum of all colored sections) of the histogram. However, an observational bias exists for the B-class flares, namely very few are identified in periods around the solar maximum due to overall reduction of detection of faint events. For this reason, B-class flares will not be considered in the quantitative analysis.

The percentage change for the entire flare population and for the sub-samples of given flare class is summarized in Table 2. The total number of flares during the ongoing SC24 is less by about one third. This value is consistent with the values obtained for the different flare classes within the uncertainty range. The overall behavior ('All' flares) is practically the same as for the C-class flares which are the most numerous group dominating the behavior of all flares. The mean/median values of the different flare class groups are very close; however the M and X-class flare samples are statistically the same, whereas the C-class flares are different in SC23 and SC24, according to the Bayesian test.

The total number of CMEs over the same 20-year period is also given in Figure 5. For the CME events we use the LASCO CME catalog that is (by August 2016) updated by the end of October 2015. This is the (additional) reason for the drop of events in the second half of year 2015 (last bin in the lower plot in Figure 5). Since 1996 the catalog has about 26 600 entries of individual CMEs. We use the reported linear (projected) CME speed. The fraction of CMEs with speed greater than 250 km/s (relevant as SEP origin

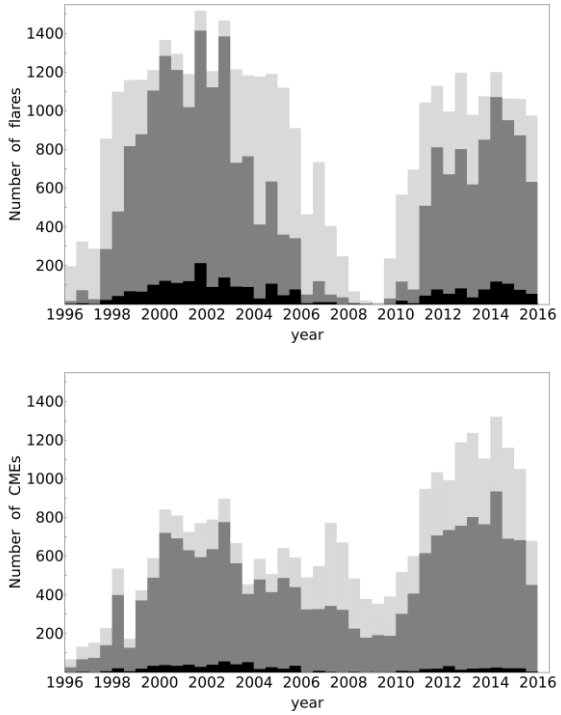

Figure 5: Distribution of the number of flares (upper) and CMEs (lower) with the solar cycle, in a 6-month time bin. The length of the color bar gives the number of events in each category. Color code: light-gray for B-class flares/V_{CME} <250 km/s, dark-gray for C-class flares/250≤V_{CME}<1000 km/s, black for M+X-class flares/V_{CME}≥1000 km/s, respectively.

candidates) constitutes 70% of the entire CME catalog with reported CME speed. The similar stacked histogram presentation is used, where the black color denotes fast (≥ 1000 km/s), gray is for intermediate speeds (in the range 250–1000 km/s) and light-gray is used for the slow CMEs (< 250 km/s). In Table 2 we summarize the number of events, mean/median values and the percentage change for all CME events and for the so-defined sub-samples. The statistical difference is confirmed only for the sample of intermediate speed CMEs, which is the most numerous sub-group (similar to the C-class flares). The mean/median values of the intermediate CME sample in SC23 show faster CMEs compared to the sample in SC24.

The total number of CMEs during SC24 increases by about 60% compared to SC23, which is similar to the increase for CMEs with speed <1000 km/s (66±2%). CMEs with projected speed of below 250 km/s in SC24 are about three times more numerous compared to SC23, whereas the CMEs with intermediate speed (between 250 and 1000 km/s) increase by about one third. In contrast to these two populations, the fast CMEs (with speeds greater than 1000 km/s) show a decrease in SC24 of about 45% that is consistent with the value found for the X-class flares. There is, however, a large data gap in 1998 due to SOHO loss and together with other gaps in the data, they introduce some observational reduction in the number of CMEs in SC23.

3.2.1 Short-time variations

The detailed plots of the percentage change for the flare and CME productivity is calculated using 6-month binning (or 14 bins in total) and the value is given at the end of the respective bin. The results are shown in Figure 6 with circles. Due to the larger data samples we use shorter time periods to outline the percentage change trends. The averaged values (as in Table 2) are shown with dotted line on each plot. The trends for all flares and for C-class flares are practically the same, with individual values all below the 0-level. There are occasional large variations in the trends, like the sudden drop at about 2 years after SC24 onset for all, M and C-class flare samples. The X-class flares show a sudden increase 3 years after the start of SC24 which is however not significant due to the large error bars. Similar increase is noticed at 6.5 year mark for X and M-class flares. The trends shown by the cumulative change (calculated in this case using 1-year step from the SC onset) in overall follows the above trends, however the behavior is smoother. The uncertainties are also smaller (and not easily seen due to the large plot range used). In about 4 years after the SC24 onset the trends reach the value for the percentage change calculated over the entire 7-year period.

The same procedure is followed while calculating the cumulative percentage change for all, fast, intermediate and slow CME samples (Figure 6). The values are given with diamond symbol in the figures. In order to calculate cumulative changes, we used the same procedure as for the SEP and flare samples. Namely, we summed the number of observed events during: only the first, first and second years, etc., finally summing up to all seven years after the SC onset. The trends for all, intermediate and slow CMEs are exclusively positive, whereas the fast CMEs show a negative trend.

While comparing the individual 6-month periods from each SC to each other, we dropped three of all 14 time bins. The last 6-month bin of the 7-year period in SC24 is excluded due to incomplete reports in November and December 2015. We also dropped bins 4 and 5, each containing large data gap in SC23 due to SOHO loss. Bin 5 contains an additional data gap from late December 1998 to early of February 1999. Thus, we present the temporal variation only over 11 bins containing complete 6-month data coverage (although occasional data gaps are present). The trends for the samples of all, fast, intermediate and slow CMEs are shown in Figure 6 with circles in the respective plots. The percentage change values for all and slow CMEs are positive, whereas the fast CME group shows negative values and/or around the 0. For the intermediate CME sample we have on average a positive trend with occasional drop in the CME productivity in some of the time bins. The behavior of all CME events follows the trend of the intermediate in speed CMEs, the latter shifted to lower values.

We calculated the values of the individual percentage change only from these 11 bins and compared them to the values obtained using the entire sample (Table 2). Using the reduced CME sample we obtain 56±2% for all (compared to +61±2%), –47±5% for fast (compared to –46±5%), +23±2% for intermediate (compared to +33±2%) and +190±10% for slow CMEs (compared to +199±9%), respectively. The differences between the two evaluations (considering or not the data gaps) are significant within the error bars for the intermediate and marginally for all CME samples. When averaged over the entire period of 7 years, the effect of the data gaps in SC23 (in 1998/1999) is to some extent minimized by the data gap in SC24 (November–December 2015). On shorter time scales, however, the presence of data gaps leads to erroneous trends in the percentage change.

Table 2: Properties of flare and CME events for different ranges of the flare class and CME speed, respectively, during the first 7 years in SC23 and SC24. The mean/median values for the flares and CMEs are calculated over the total number of events in each category (given in brackets).

Categories of solar eruptive events	Mean/Median SC23: 09/1996-08/2003	Mean/Median SC24: 01/2009-12/2015	Statistical difference	Change in SC24
C-to-X flares				–34±1 %
• X-class	X2.6/X1.7 (80)	X2.0/X1.7 (45)	No	–44±10 %
• M-class	M2.3/M1.6 (1112)	M2.4/M1.6 (694)	No	–38±3 %
• C-class	C3.0/C2.4 (10889)	C2.7/C2.0 (7266)	Yes	–33±1 %
CMEs				+61±2 %
• ≥ 1000 km/s	1297/1183 (349)	1309/1195 (187)	No	–46±5 %
• 250– 1000 km/s	497/459 (6017)	423/380 (8029)	Yes	+33±2 %
• < 250 km/s	186/195 (1455)	184/191 (4346)	No	+199±9 %

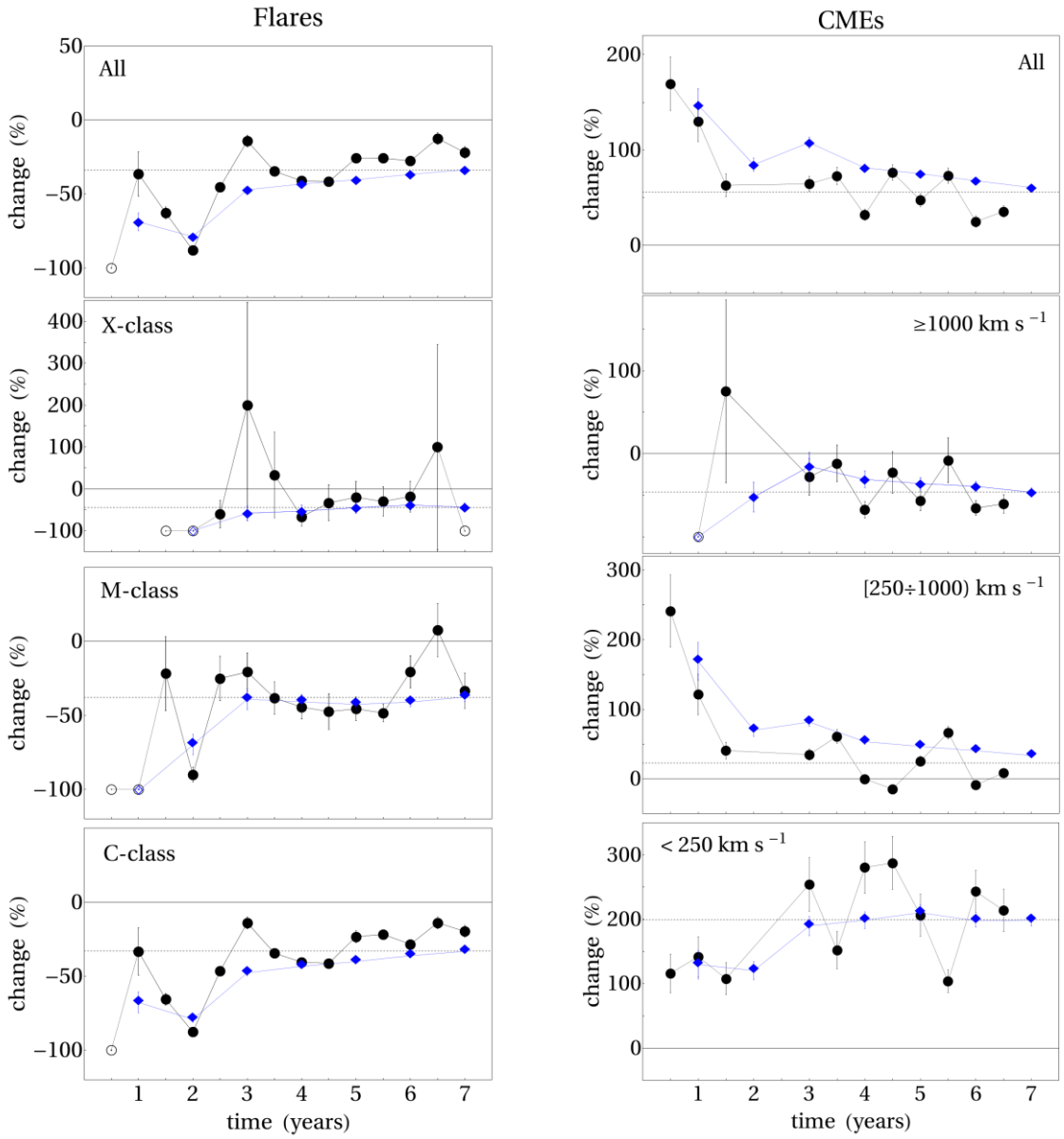

Figure 6: Plots of the 6-month percentage change (black circles) and cumulative percentage change (blue diamonds) for flares (left) and CMEs (right). Positive (negative) values denote more (less) events in SC24 compared to SC23. Empty symbols denote a percentage change value with undetermined uncertainty due to empty bins in SC24. The dotted line in all plots is the respective value averaged over all 7 years (see Table 2).

4. Summary and discussion

In the present study we focus on the overall samples of SEP, flare and CME events in SC23 and SC24. We obtain a drop of the entire sample of Wind/EPACT proton events (both at 25 and 50 MeV) in the ongoing SC24 by about –30%. The reduction is less for minor (of about –20%) and more for major proton events (the drop is in the range between –60% and -100%, with larger decrease for the high energy protons). A reduction value of about –32% is reported by Mewaldt et al. (2015) for GOES >10 MeV SEP events. A decrease of the number of protons in SC24 is also reported by Gopalswamy (2012) and Chandra et al. (2013), see their Tables 3.

In our study we find that the reduction of proton events in SC24 compared to SC23 is consistent with the reduction trends obtained for X-to-C-class flares (in the range between –33 to –44%) and fast CMEs (–46%) over the same equivalent periods of time. The slow CME events, with speeds below 1000 km/s, are more numerous in SC24 (increase of 66%) in contrast to the overall drop in the occurrence rate of SEP events. The percentage change varies slightly on a shorter time periods compared to the averaged value. SC24 started with a larger number of CMEs compared to the SC23 onset followed by a significant drop in productivity in the first 1.5 years. This is due to the larger number of CME events reported during the last solar

minimum, compared to the previous minimum period. For the flares, the trends start at –100% level, since no C, M, X-class flares were observed during the 0.5, 1, 2-year period after the start of SC24, respectively. Short-term variations are not significant due to the large uncertainty and could be in fact an artifact of the low sampling.

For the Wind/EPACT protons, we obtain a short period of increased proton productivity only during 2012 for the ~25 MeV protons with peak intensity 0.1-10 $(cm^2\ s\ sr\ MeV)^{-1}$ compared to the otherwise weak SC24 proton productivity. Although, similar trend is observed for other proton events in the two energy channels the uncertainty is too large to be conclusive.

In the present study, we considered the entire populations of solar eruptive events over nearly two SC. The SEP-productive flares and CMEs in SC24 will ultimately stem from these flare/CME populations, shown to contain a reduced fraction of large events, compared to SC23. The lack of strong events expected to form the bulk of the efficient particle acceleration drivers is consistent with our finding of a reduced number of SEP events observed in SC24. This is also consistent with the results presented by Mewaldt et al. (2015) who obtained a reduced number of seed particles in SC24 based on particle composition analysis. The overall properties of the Wind/EPACT proton-productive flare and CME populations are beyond the scope of this study.

In summary, our results confirm that the ongoing SC24 is poor in 25–50 MeV proton events, X-to-C class solar flares and faster than 1000 km/s CMEs. All these phenomena are reduced on average by 30–45%. Occasionally, short-time variability in the productivity trends are noticed, which could be due to small-scale offset in the productivity rate between the two SCs. Large data gaps can introduce a bias into the short-time trends and interpretations, as it was shown to be the case for the CMEs, but the effect is smoothed out over large periods of time.

Acknowledgements

We acknowledge the open data policy for the SEP data and flare and CME catalogs. The CME catalog is generated and maintained at the CDAW Data Center by NASA and The Catholic University of America in cooperation with the Naval Research Laboratory. SOHO is a project of international cooperation between ESA and NASA. Sunspot data is from the World Data Center SILSO, Royal Observatory of Belgium. RM thanks T. Dudok de Wit for the valuable discussion. MVCD thanks a support by FAPESP (process number 2014/18632-6). This project has received funding from the European Union's Horizon 2020 research and innovation programme under grant agreement No. 637324.

References

Agueda, N., Klein, K.-L., Vilmer, N., et.al.: 2014, Astron. Astrophys. 570, A5 DOI: 10.1051/0004-6361/201423549

Cane, H.V., Richardson, I.G., von Rosenvinge, T.T.: 2010, J. Geophys. Res. (Space Physics) 115, A8, CiteID A08101 DOI: 10.1029/2009JA014848

Chandra, R., Gopalswamy, N., Mäkelä, P., et.al.: 2013, Adv. Space Res. 52, 2102 DOI: 10.1016/j.asr.2013.09.006

Gomez-Herrero, R., Dresing, N., Klassen, A., et.al.: 2015, Astrophys. J. 799, id. 55, 17 pp. DOI: 10.1088/0004-637X/799/1/55

Blanco, J.J., Rodríguez-Pacheco, J., Banjac, S.: 2015, Astrophys. J. 799, id. 55, 17 pp. DOI: 10.1088/0004-637X/799/1/55

Gopalswamy, N.: 2012, in Q. Hu, G. Li, P. Zank, G. Fry, X. Ao, and J. Adams (eds.), Space Weather: The Space Radiation Environment: 11th Annual International Astrophysics Conference, AIP conference proceedings 1500, Issue 1, p. 14 DOI: 10.1063/1.4768738

Gopalswamy, N., Yashiro, S., Michalek, G., et.al.: 2009, Earth, Moon, and Planets, 104, 295 DOI: 10.1007/s11038-008-9282-7

Gopalswamy, N., Xie, H.S. Akiyama S., Mäkelä, P.A., Yashiro, S.: 2014, Earth, Planets and Space, 66: 104, 15 pp. DOI: 10.1186/1880-5981-66-104

Hathaway, D.H.: 2010, Living Reviews in Solar Physics 7, 1, http://www.livingreviews.org/lrsp-2010-1 DOI: 10.12942/lrsp-2010-1

Huttunen-Heikinmaa, K., Valtonen, E., Laitinen, T.: 2005, Astron. Astrophys. 442, 673 DOI: 10.1051/0004-6361:20042620

Kaiser, M.L., Kucera, T.A., Davila, J.M., et.al.: 2008, Space Sci. Reviews 136, 5 DOI: 10.1007/s11214-007-9277-0

Klein, K.-L., Krucker, S., Lointier, G., Kerdraon, A.: 2008, Solar Phys. 486, 589 DOI: 10.1051/0004-6361:20079228

Krucker, S., Larson, D.E., Lin, R.P., Thompson, B.J.: 1999, Astrophys. J. 519, 864 DOI: 10.1086/307415

Kruschke, J. K.: 2013, J. Experimental Psychology: General, 142, 573 DOI: 10.1037/a0029146

McComas, D.J., Angold, N., Elliot, H.A., et.al.: 2013, Astrophys. J. 779, id. 2, 10 pp. DOI: 10.1088/0004-637X/779/1/2

Mewaldt, R.A., Cohen, C.M.S., Mason, G.M., et.al.: 2015, in Proc. Inter. Cosmic Rays Conference

Miteva, R., Klein, K.-L., Malandraki, O., Dorrian, G.: 2013, Solar Phys. 282, 579 DOI: 10.1007/s11207-012-0195-2

Miteva, R., Klein, K.-L.; Kienreich, I., Temmer, M., Veronig, A., Malandraki, O.E.: 2014, Solar Phys. 289, 2601 DOI: 10.1007/s11207-014-0499-5

Miteva, R., Samwel, S.W., Costa-Duarte, M.V., Danov, D.: 2016, in K. Georgieva, B. Kirov and D. Danov (eds.), Proc. Eighth Workshop "Solar Influences on the Magnetosphere, Ionosphere and Atmosphere", p. 27

Reames, D.V.: 2013, Solar Phys. 175, 53 DOI: 10.1007/s11214-013-9958-9

von Rosenvinge, T.T., Barbier, L.M., Karsch, J., et.al.: 1995, Space Sci. Reviews 71, 155 DOI: 10.1007/BF00751329

Schwenn, R.: 2006, Living Reviews in Solar Physics 3, http://www.livingreviews.org/lrsp-2006-2 DOI: 10.12942/lrsp-2006-2

Tylka, A.J., Cohen, C.M.S., Dietrich, W.F., et.al.: 2003, in Proc. Inter. Cosmic Rays Conference, p. 3305

Vainio, R., Valtonen, E., Heber, B., Malandraki, O.E., Papaioannou, A., Klein, K.-L., et al..: 2013, J. Space Weather and Space Climate 3, id. A12, 17 pp. DOI: 10.1051/swsc/2013030